HHS Public Access

Author manuscript

New Phytol. Author manuscript; available in PMC 2022 February 01.

Published in final edited form as:

New Phytol. 2021 August ; 231(3): 1008–1022. doi:10.1111/nph.17007.

MicroRNA156-mediated changes in leaf composition lead to altered photosynthetic traits during vegetative phase change

Erica H. Lawrence[1], **Clint J. Springer**[2], **Brent R. Helliker**[1], **R. Scott Poethig**[1]

[1]Department of Biology, University of Pennsylvania, 433 South University Avenue, Philadelphia, PA 19104, USA

[2]Department of Biology, Saint Joseph's University, 5600 City Avenue, Philadelphia, PA 19131, USA

Summary

● Plant morphology and physiology change with growth and development. Some of these changes are due to change in plant size and some are the result of genetically programmed developmental transitions. In this study we investigate the role of the developmental transition, vegetative phase change (VPC), on morphological and photosynthetic changes.

● We used overexpression of microRNA156, the master regulator of VPC, to modulate the timing of VPC in *Populus tremula* × *alba, Zea mays*, and *Arabidopsis thaliana* to determine its role in trait variation independent of changes in size and overall age.

● Here, we find that juvenile and adult leaves in all three species photosynthesize at different rates and that these differences are due to phase-dependent changes in specific leaf area (SLA) and leaf N but not photosynthetic biochemistry. Further, we found juvenile leaves with high SLA were associated with better photosynthetic performance at low light levels.

● This study establishes a role for VPC in leaf composition and photosynthetic performance across diverse species and environments. Variation in leaf traits due to VPC are likely to provide distinct benefits under specific environments; as a result, selection on the timing of this transition could be a mechanism for environmental adaptation.

Keywords

juvenile-to-adult transition; leaf nitrogen; miR156; photosynthesis; specific leaf area; vegetative phase change

Author for correspondence: *Erica H. Lawrence*, lawrence.erica.h@gmail.com.

Author contributions

EHL, CJS, BRH and RSP planned and designed the research. EHL performed the experiments. EHL performed statistical analyses and wrote the manuscript. EHL, CJS, BRH and RSP revised and provided comments on the manuscript.

Supporting Information

Additional Supporting Information may be found online in the Supporting Information section at the end of the article.

Introduction

As plants age they go through developmental transitions that impact their form and function. One of these transitions occurs as plants shift between juvenile and adult vegetative growth phases. This developmental transition is known as vegetative phase change (VPC) and has been observed across phylogenetically diverse groups of plants from mosses to angiosperms. This transition is controlled by expression levels of the highly conserved microRNA156 (miR156) and in some species the closely related miR157 (Willmann & Poethig, 2007; Axtell & Bowman, 2008; Zhang et al., 2015). miR156 and 7 are expressed at high levels in leaves produced early in development, and negatively regulate the expression of their targets, the Squamosa Promoter Binding Protein-Like (*SPL*) transcription factors. Expression of miR156 and 7 declines later in development, alleviating the transcriptional and translational repression of these *SPL* genes. This increase in *SPL* expression promotes adult vegetative traits, leading to VPC (Wu & Poethig, 2006; Wu et al., 2009; Wang et al., 2011; Xu et al., 2016; He et al., 2018). The traits that change during VPC are species dependent, but they broadly include changes in leaf morphology, growth rate, growth form, and reproductive competence (Poethig, 1990; Bassiri et al., 1992; Bongard-Pierce et al., 1996; Telfer et al., 1997; Wang et al., 2011; Feng et al., 2016; Leichty & Poethig, 2019; Silva et al., 2019).

How plants respond to dynamic challenges in their environment varies with age (Cavender-Bares & Bazzaz, 2000; Niinemets, 2010; Kitajima et al., 2013; Hahn & Orrock, 2016) and has important implications for plant community composition, the competitive ability of different species, and their response to future climate change (Parish & Bazzaz, 1985; Lamb & Cahill, 2006; Moll & Brown, 2008; Piao et al., 2013; Spasojevic et al., 2014; Kerr et al., 2015; Lasky et al., 2015). For example, seedlings are particularly vulnerable to factors such as shading, drought, disturbance, and herbivory (Kabrick et al., 2015; Charles et al., 2018), and they often experience a high rate of mortality (Grossnickle, 2012). Species that are able to transition to a more resilient phase for their environment are likely to have a competitive advantage. Although it is reasonable to assume that VPC plays an important role in this process, how VPC affects the response of plants to various biotic and abiotic stresses is still poorly understood.

Defining the role of VPC in plant physiology is difficult because this transition occurs concurrently with changes in plant size and age. Juvenile leaves and branches are produced on smaller plants than adult organs and, thus, are exposed to different amounts and types of endogenous factors (e.g. hormones, carbohydrates). Furthermore, light, temperature, and humidity vary according to position within the canopy and proximity to the ground (Evans & Coombe, 1959; Waggoner & Reifsnyder, 1968; Shuttleworth et al., 1985; Canham, 1988; Canham et al., 1994; Still et al., 2019), meaning that juvenile and adult organs exist in different microclimates. Finally, the temporal separation between the production of juvenile and adult organs means that seasonal changes in environmental conditions also contribute to age-dependent differences in physiological traits. These problems can only be addressed by varying the timing of VPC under controlled environmental conditions, independent of shoot growth.

The importance of various leaf traits – including photosynthetic traits, specific leaf area (SLA), leaf nitrogen (N) content, and gas exchange – for plant growth and survival have been well documented (Lusk & Del Pozo, 2002; Poorter & Bongers, 2006; Modrzynski et al., 2015). Previous studies have shown that photosynthetic genes are differentially expressed in juvenile and adult maize (*Zea mays*) leaves (Strable et al., 2008; Beydler, 2014), but comparisons of various photosynthetic traits in these leaves have produced inconclusive and sometimes conflicting results (Bond, 2000; Steppe et al., 2011; Sun et al., 2018; Kuusk et al., 2018a, b). The basis for these inconsistencies is unclear, but the compounding effects of variation in plant size, leaf age, environment, and time of year are possibilities (Bauer & Bauer, 1980; Bond, 2000; Ishida et al., 2005; Velikova et al., 2008; Steppe et al., 2011). Although these effects can be minimized through techniques such as grafting, *in vitro* rejuvenation, and pruning (Hutchison et al., 1990; Huang et al., 2003; Kubien et al., 2007; Jaya et al., 2010), these methods do not completely distinguish the effect of VPC from other factors that may contribute to these differences. For example, grafting old shoots to young roots is often used to determine if a trait is dependent on plant size. However, miR156 is a mobile microRNA and can move across a graft junction (Marin-Gonzalez & Suarez-Lopez, 2012; Bhogale et al., 2014; Ahsan et al., 2019; Fouracre & Poethig, 2019), so this approach does not necessarily eliminate the effect of this key regulator of vegetative identity. Similarly, the methods that are typically used to induce vegetative rejuvenation (*in vitro* culture, pruning) affect both the level of miR156 (Irish & Karlen, 1998; Li et al., 2012) and plant size.

We used overexpression of miR156 in three species – *Populus tremula* × *alba, Z. mays*, and *Arabidopsis thaliana* – to delay the timing of VPC, allowing us to differentiate traits associated with this developmental transition from those regulated by plant size or age. Our results demonstrate that juvenile leaves are photosynthetically distinct from adult leaves and that this difference can be attributed primarily to the morphological differences between these leaves, not to a fundamental difference in the biochemistry of photosynthesis.

Materials and Methods

Plant material

Populus tremula × *alba* line 717-1B4 and two independent miR156 overexpressor lines, 40 and 78, described in Lawrence et al. (2020), were obtained by *in vitro* propagation and hardened on propagation media as described in Meilan & Ma (2006). Plants were then transplanted to Fafard-2 growing mix (Sun Gro Horticulture, Agawam, MA, USA) in 0.3 l pots in a glasshouse at the University of Pennsylvania (39.9493°N, 75.1995°W, 22.38 m above sea level (asl)) and kept in plastic bags for increased humidity for 2 wk. Plants were transferred to 4.2 l pots with Fafard-52 growing mix 3 wk later and fertilized with Osmocote 14-14-14 (The Scotts Company, Marysville, OH, USA). Plants were additionally fertilized once a week with Peters 20-10-20 (ICL Fertilizers, Dublin, OH, USA). Glasshouse conditions consisted of a 16 h photoperiod with temperatures between 22 and 27°C. Light levels were based on natural light and supplemented with 400 W metal halide lamps (P.L. Light Systems, Lincoln, ON, Canada) with daily irradiances between 300 to 1500 μmol m^{-2}

s^{-1} across the day. All settings were controlled by Priva (Vineland Station, ON, Canada) and Microgrow (Temecula, Canada) glasshouse systems.

Populus tremula × alba seeds from Sheffield's Seed Company (Locke, NY, USA) were germinated on a layer of vermiculite on top of Fafard-2 growing mix in 0.64 l pots in a glasshouse under the conditions already described herein. Seedlings were transplanted to 1.76 l pots with Fafard-52 growing mix with Osmocote 14-14-14 at 1 month after germination and were then transplanted to 4.2 l pots 3 months following the previous transplant.

Zea mays seeds with the *Corngrass 1* (*Cg1*) mutation (stock 310D) – which consists of a tandem duplication of miR156b/c primary sequences described in Chuck et al. (2007) – and the W22 inbred line were obtained from the Maize Genetics Cooperation Stock Center (Urbana, IL, USA). Plants heterozygous for *Cg1* were crossed to W22 to produce the *Cg1/+* and +/+ siblings used in this study. Seeds were planted in 9.09 l pots with Fafard-52 growing mix and fertilized with Osmocote 14-14-14 in a glasshouse under growing conditions already described herein.

Arabidopsis thaliana (Col) and the 35S:miR156 overexpressor line described in Wu & Poethig (2006) were planted in 0.06 l pots with Fafard-2 growing mix as described by Flexas et al. (2007). Beneficial nematodes (*Steinernema feltiae*; BioLogic, Willow Hill, PA, USA), Marathon® 1% granular insecticide and diatomaceous earth were added to the growing mix to control insects. Planted seeds were placed at 4°C for 3 d before being grown at 22°C in Conviron growth chambers under short days (10 h : 14 h, light : dark) at 60 μmol m^{-2} s^{-1} light to obtain leaves large enough to fit in the gas-exchange chamber. Plants were fertilized with Peters 20-10-20 every other week.

Individuals from genotypes of all species were positioned in a randomized fashion in the glasshouse and rotated frequently. Planting was staggered across two, three and five months for *Arabidopsis, P. tremula* × *alba*, and *Z. mays*, respectively.

Leaf samples

All measurements and sampling were conducted on the uppermost fully expanded leaf. In *P. tremula* × *alba* 717-1B4 and miR156 overexpressor lines, leaves 10, 15, 20, and 25 were measured. Leaves 10 and 15 in the wild-type 717-1B4 line were juvenile and leaves 20 and 25 were adult, as determined by petiole shape and abaxial trichome density as described in Lawrence et al. (2020). All leaves measured in the miR156 overexpressor lines were juvenile. Leaves 1–52 were measured in poplar plants germinated from seed. The juvenile-to-adult transition in these plants occurred between leaves 20 and 30, as determined by the change in petiole shape and trichome density (Lawrence et al., 2020). In *Z. mays*, leaves 2–11 were measured with leaves 1–5 juvenile in wild-type plants and all leaves juvenile in *Cg1* mutants. Developmental stage in maize was determined by the presence or absence of epicuticular wax and trichomes as described in Poethig (1988). In *A. thaliana*, leaves 5 and 10 were measured. In wild-type plants, leaf 5 was juvenile and leaf 10 was adult, as determined by the presence or absence of abaxial trichomes. All leaves were juvenile in miR156 overexpressors. Throughout this paper, 'juvenile' and 'adult' refer to naturally

juvenile or adult leaves in wild-type lines, and 'juvenilized' refers to leaves in miR156 overexpressor lines that have a juvenile phenotype at leaf positions that would normally be adult. The phenotypes of fully expanded adult, juvenile, and juvenilized leaves of *P. tremula* × *alba*, *A. thaliana*, and maize are shown in Fig. 1.

Gas-exchange measurements

All gas-exchange measurements were made using an Li-6400 portable photosynthesis machine (Li-Cor Environmental, Lincoln, NE, USA) at a leaf temperature of 25°C following acclimatization to starting chamber conditions. Photosynthetic capacity in *A. thaliana* was measured using steady-state net photosynthesis (A_{net})–intercellular [CO_2] (C_i) curves by measuring A_{net} at reference [CO_2] of 400, 200, 50, 100, 150, 200, 250, 300, 600, 800, 1000, and 1200 ppm, at an air flow rate of 300 μmol s^{-1}, minimum wait time of 2 min, and light level of 1000 μmol m^{-2} s^{-1}. *Zea mays* A_{net}–C_i curves measured A_{net} at reference [CO_2] of 400, 350, 300, 250, 200, 150, 100, 50, 400, 500, 600, 700, 800, 1000, 1200 ppm, at an air flow rate of 400 μmol s^{-1}, minimum wait time of 2 min, and light level of 1800 μmol m^{-2} s^{-1}. Photosynthetic capacity in *P. tremula* × *alba* was measured using rapid A_{net}–C_i response (RACiR™) curves as described in Lawrence et al. (2019). Briefly, A_{net} was measured from reference [CO_2] of 300 to 800 μmol m^{-2} s^{-1} at 60 μmol mol^{-1} min^{-1} CO_2 and a light level of 1500 μmol m^{-2} s^{-1}. This technique was used to expedite measurements after development of the RACiR technique for the Li-6400 showed no significant differences from steady-state A_{net}–C_i curves.

Light-response curves were performed in all three species at a reference [CO_2] of 400 ppm. A_{net} was measured at light levels of 1000, 800, 600, 300, 200, 150, 100, 75, 50, 25, and 0 μmol m^{-2} s^{-1} in *A. thaliana*, 1800, 1500, 1200, 1000, 800, 600, 300, 200, 150, 100, 75, 50, 25 and 0 μmol m^{-2} s^{-1} in *Z. mays*, and 1500, 1200, 1000, 800, 600, 300, 200, 150, 100, 75, 50, 25, 10 and 0 μmol m^{-2} s^{-1} in *P. tremula* × *alba.* Flow rate, leaf temperature, and minimum wait times were the same as for A_{net}–C_i curves.

The low-light photosynthetic rates $A_{low\ light}$ shown in Fig. 7 were obtained by averaging photosynthetic rates over a 2 min period at light levels approximately two to three times the light compensation point. These values were 25 μmol m^{-2} s^{-1} in *P. tremula* × *alba* and *A. thaliana* and 50 μmol m^{-2} s^{-1} in *Z. mays.* All leaves were acclimated to the chamber conditions before measurements began, and flow rate and leaf temperature were consistent with previously described measurements.

Daytime respiration rates were determined by averaging A_{net} at 0 μmol m^{-2} s^{-1} irradiance over a 1 min period after the leaves were dark adapted for 1 h.

Leaf fluorescence

Light and dark-adapted fluorescences were determined using an Li-6400 equipped with fluorometer head. Light-adapted measurements were taken using a multiphase flash with a 250 ms phase 1, 500 ms phase 2 with a 20% declining ramp and 250 ms phase 3 after leaves acclimated to saturating light values of 1000 μmol m^{-2} s^{-1}, 1800 μmol m^{-2} s^{-1} and 1500 μmol m^{-2} s^{-1} for *A. thaliana, Z. mays* and *P. tremula* × *alba*, respectively. Dark-adapted

fluorescence measurements were taken using an 800 ms saturating rectangular flash after dark-adapting leaves for 1 h.

Leaf nitrogen, Chl, and specific leaf area

Leaf tissue was sampled after gas exchange; one subsample for each leaf was dried at 60°C until constant mass to determine SLA. Dried tissues were ground using a mortar and pestle. Leaf N was measured in the dried samples using an ECS 4010 CHNSO Analyzer (Costech Analytical Technologies Inc., Valencia, CA, USA). A second subsample was frozen and used for Chl quantification. Chl was extracted using 80% acetone and quantified using a spectrophotometer according to equations found in Porra et al. (1989).

Leaf cross-sections

Fresh leaf tissue from the middle of fully expanded leaves at positions 5 and 10 of *A. thaliana*, 10 and 25 of *P. tremula* × *alba*, and 4 and 11 of *Z. mays* in both wild-type and miR156 overexpressor lines was cut and fixed with a 10× formalin–propionic acid–glycerol–95% ethanol solution overnight. Samples were then washed with 50% ethanol and dehydrated through an ethanol/*tert*-butyl alcohol (TBA) series with 2 h incubations at room temperature for each step. Sections in 100% TBA were subsequently transferred to Paraplast Plus embedding medium at 60°C and incubated for 48 h. Embedded samples were set in molds and cut into 12 μm sections using a microtome. Samples were floated on 0.01% Sta-on on glass slides and dried at 40°C. Samples were then deparaffinized in xylenes and rehydrated through an ethanol series for staining with 1% Safranin O in 50% ethanol and subsequent dehydrating for staining with 0.1% Fast green in 95% ethanol. Once fully stained and dehydrated, sections were mounted in permount and visualized and photographed using an Olympus BX51 light microscope and DP71 digital camera.

Curve fitting

The PLANTECOPHYS package in Duursma (2015) was used for fitting A_{net}–C_i curves to determine V_{cmax} and J_{max} using the bilinear function for *A. thaliana* and *P. tremula* × *abla.* The C_4 photosynthesis estimation tool presented in Zhou et al. (2019) based on Yin et al. (2011) was used for fitting A_{net}–C_i curves for *Z. mays.*

Light-response curves were analyzed using the AQ_CURVES curve-fitting script in R (Tomeo, 2019), which uses equations based on a standard nonrectangular hyperbola model fit described in Lobo et al. (2013).

Data analysis

All statistical analyses were performed in JMP® PRO v.14.0.0 (SAS Institute Inc., Cary, NC, USA). Gas exchange and leaf composition traits between adult, juvenile, and juvenilized leaves were compared by one-way ANOVA, where developmental stage was the main effect and *P*-values were corrected for multiple testing within a species using false-discovery rate (FDR). When ANOVA results were significant ($P < 0.05$) a Student's *t*-test was performed to determine differences between developmental groups. Traits were considered to be affected by developmental phase when adult leaves were significantly different from both juvenile and juvenilized leaves with the same trend. The effect of leaf position on measured traits was

determined by two-way ANOVA with leaf position and genotype as the main effects and *P*-values corrected using FDR. Because developmental phase and leaf position are coordinated in wild-type plants, many traits affected by development showed significant leaf position effects ($P < 0.05$). Of these traits, those that showed no significant interaction between leaf position and genotype, indicating there were no significant differences between wild-type and miR156 overexpressor plants that do not produce adult leaves, are affected by leaf position independent of leaf developmental stage. Photosynthetic N use efficiency was determined using least-squares linear regression analysis across all leaves and was compared by ANCOVA with developmental stage as the covariate. The relationships between A_{sat} and leaf N or SLA were determined using least-squares linear regression analysis.

Results

Photosynthetic rates differ between juvenile and adult leaves

The rate of light-saturated area-based photosynthesis $A_{sat\ Area}$ was significantly different in juvenile and adult leaves of *P. tremula* × *alba* and *A. thaliana* but was not significantly different in maize (Fig. 2a–c). Adult leaves in *P. tremula* × *alba* had a 26% greater $A_{sat\ Area}$ (15.56 μmol m^{-2} s^{-1}) than their juvenile counterparts did (12.28 μmol m^{-2} s^{-1}), whereas the adult leaves in *A. thaliana* had a 57% greater $A_{sat\ Area}$ (8.13 μmol m^{-2} s^{-1}) than juvenile leaves did (5.18 μmol m^{-2} s^{-1}). The phase dependence of this difference was confirmed by the phenotype of lines overexpressing miR156. The $A_{sat\ Area}$ of adult leaves in *P. tremula* × *alba* was, respectively, 104% and 105% greater than the $A_{sat\ Area}$ of the corresponding juvenilized leaves in lines 40 (7.57 μmol m^{-2} s^{-1}) and 78 (7.54 μmol m^{-2} s^{-1}), whereas the $A_{sat\ Area}$ of adult leaves in *Arabidopsis* was 42% higher than that of juvenilized leaves (5.73 μmol m^{-2} s^{-1}).

Mean mass-based photosynthetic rates $A_{sat\ Mass}$ were lower in adult leaves than in juvenile leaves in all three species, although this difference was only statistically significant in maize (Fig. 2d–f). In maize, juvenilized leaves had essentially the same $A_{sat\ Mass}$ as normal juvenile leaves, suggesting that the difference in $A_{sat\ Mass}$ between juvenile and adult leaves is phase dependent. However, the $A_{sat\ Mass}$ of juvenilized leaves in *P. tremula* × *alba* and *A. thaliana* was significantly lower than that of juvenile leaves and was more similar to that of adult leaves.

Leaf morphology and composition is phase dependent

Inconsistencies in the relationship between leaf identity and A_{sat} on an area or mass basis across species suggests that leaf-to-leaf variation in the rate of photosynthesis is either determined by variation in the leaf area/mass relationship or by variation in the photosynthetic biochemistry in these species. *Populus tremula* × *alba* and *A. thaliana* both undergo C_3 photosynthesis, whereas maize is a C_4 plant, so it is reasonable to assume that the factors contributing to developmental variation in photosynthesis in these species could be quite different. To address this issue, we measured morphological, chemical, and physiological traits in adult, juvenile, and juvenilized leaves of these species.

SLA represents the amount of area per unit of leaf mass and is a proxy for the thickness or density of the leaf blade; in general, leaves with a high SLA are thinner than leaves with a low SLA. Adult leaves of all three species had a significantly lower SLA than juvenile leaves (Fig. 3a–c). Furthermore, the SLA of juvenilized leaves was significantly higher than that of adult leaves and was similar, if not identical to, the SLA of juvenile leaves in both *P. tremula* × *alba* and maize. This result suggests that SLA is phase dependent in all three species. Although we did not conduct a detailed quantitative analysis of the basis for the difference in SLA between juvenile and adult leaves, cross-sections of the leaf blade suggest that this difference is attributable to a combination of variation in both leaf thickness and tissue density, with the relative importance of these traits differing in different species (Fig. 4). Consistent with their SLA, the anatomy of juvenilized leaves of *P. tremula* × *alba* and *Arabidopsis* appeared to be intermediate between that of juvenile and adult leaves, whereas juvenilized leaves in maize more closely resembled normal juvenile leaves than adult leaves.

The relationship between leaf N and phase identity varied depending on whether this trait was measured on an area or mass basis and was similar to the results obtained for photosynthetic rates. Measured on a mass basis, leaf N was not significantly different in juvenile and adult leaves of *P. tremula* × *alba* or *A. thaliana* and was not significantly different between juvenilized and adult leaves of these species. However, in maize, leaf N/mass was significantly lower in adult leaves than in either juvenile or juvenilized leaves (Fig. 3d–f). Thus, leaf N/mass is a phase-dependent trait in maize but not in *P. tremula* × *alba* or *A. thaliana.* The opposite result was obtained when leaf N was measured as a function of leaf area. The leaf N/area in both *P. tremula* × *alba* and *A. thaliana* was significantly higher in adult leaves than in juvenile or juvenilized leaves, implying that it is phase dependent in these species. However, there was no significant difference in the leaf N/area of adult, juvenile, or juvenilized leaves in maize (Fig. 3g–i).

SLA and leaf N were significantly correlated with phase-dependent photosynthetic rates ($A_{\text{sat Area}}$ in *P. tremula* × *alba* and *A. thaliana*; $A_{\text{sat Mass}}$ in maize) in all three species (Fig. 5; Supporting Information Table S1). SLA was negatively correlated with $A_{\text{sat Area}}$ in *P. tremula* × *alba* and *A. thaliana* and positively correlated with $A_{\text{sat Mass}}$ in *Z. mays.* This negative relationship was weaker in *P. tremula* × *alba* ($r^2 = 0.167$) likely because of low g_s in the juvenilized leaves (Table S2) leading to lower than wild-type A_{sat}. When juvenilized leaves were excluded from the analysis, a stronger but similar linear fit existed among the adult and juvenile wild-type leaves ($A_{\text{sat}} = 24.11 - 0.02255 \times \text{SLA}$, $r^2 = 0.436$, $P < 0.0001$). Leaf N is positively correlated with $A_{\text{sat Area}}$ in *P. tremula* × *alba* and *A. thaliana* and $A_{\text{sat Mass}}$ in *Z. mays.* However, photosynthetic N use efficiency (PNUE), calculated as the relationship between A_{sat} and leaf N, did not vary based on leaf developmental phase (Table 1).

We also compared Chl*a* and *b* (Chl*a*+*b*) levels and ratios between adult, juvenile, and juvenilized leaves. Chl*a* + *b* was not significantly different across leaves of different developmental phases. However, the Chl*a* : Chl*b* ratio was phase dependent in *P. tremula* × *alba* and *Z. mays* (Table S2). Changes in Chl*a* : Chl*b* ratios followed the same trends as leaf N, with lower ratios in juvenile and juvenilized leaves than in adult leaves of *P. tremula* ×

alba and the opposite in *Z. mays.* As Chl*a* is associated with more proteins than Chl*b* is, these data support one another.

There were no phase-dependent differences in stomatal conductance g_s or daytime respiration R_{day} between adult and juvenile or juvenilized leaves in any of the test species (Table S2).

To determine if phase-dependent variation in A_{sat} is attributable to variation in the biochemistry of photosynthesis, we examined traits modeled from A_{net}–C_i curves (V_{cmax}, maximum Rubisco carboxylation rate; J_{max}, maximum electron transport rate for ribulose-1,5-bisphosphate regeneration; Fig. 6), traits modeled from light-response curves (Φ, quantum yield; LCP, light compensation point), and traits modeled from dark and light-adapted fluorescence (F_v/F_m, maximum quantum efficiency of photosystem II (PSII); F'_v/F'_m, maximum operating efficiency; ΦPSII, quantum yield of PSII; NPQ, nonphotochemical quenching; ETR, electron transport rate). With one exception, none of these traits was significantly different between adult and juvenile/juvenilized leaves. The sole exception was F_v/F_m in *P. tremula* × *alba*, which was 6.3% higher in adult leaves than in juvenile leaves (Table S2). When V_{cmax}, J_{max}, and ETR were converted to mass-based measures using SLA, ETR_{Mass} in *Z. mays* was the only trait determined to be phase dependent with juvenile and juvenilized leaves, having rates of 2.24 μmol g^{-1} s^{-1} and 3.18 μmol g^{-1} s^{-1} faster than adult leaves, respectively (Table S2). It is possible these differences in ETR contribute to the phase-dependent differences observed in $A_{sat\ Mass}$. However, the lack of phase dependence in ΦPSII and J_{max} suggest otherwise.

The observation that phase-dependent variation in A_{sat} is correlated with SLA and leaf N but not with most measures of photosynthetic or physiological efficiency suggests that phase-dependent aspects of leaf anatomy, as well as phase-dependent variation in leaf composition (e.g. protein content), are the primary determinants of variation in the rate of photosynthesis during shoot development.

Low-light photosynthetic traits

Under low light conditions (≤ 50 μmol m^{-2} s^{-1}), adult and juvenile/juvenilized leaves of *P. tremula* × *alba* and *A. thaliana* showed no differences in area-based photosynthetic rates $A_{low\ light\ Area}$, whereas adult leaves of *Z. mays* had a slightly, but significantly lower $A_{low\ light\ Area}$ than juvenile or juvenilized leaves (Fig. 7). This is in contrast to the relative rates of photosynthesis we observed at saturating light levels, where adult leaves of *P. tremula* × *alba* and *A. thaliana* had a significantly higher $A_{sat\ Area}$ than juvenile leaves, and the $A_{sat\ Area}$ in maize was not significantly different in these leaf types. The relative advantage of juvenile leaves under low light conditions was even more pronounced when photosynthesis was measured on a mass basis ($A_{low\ light\ Mass}$): in low light, juvenile and juvenilized leaves of all three species had a significantly higher $A_{low\ light\ Mass}$ than adult leaves did. These results suggest that juvenile leaves are better adapted for photosynthesis under low light conditions than adult leaves are.

Role of leaf position on phase-dependent traits

To determine whether there was an effect of leaf position – independent of phase identity – on various traits, we looked across all measured leaf positions in wild-type and miR156 overexpressors of *P. tremula* × *alba* and *Z. mays.* Traits that varied with leaf number but were not significantly different between wild-type and mutant plants were considered to be affected by leaf position independently of their phase identity. This is because wild-type plants had juvenile leaves at low nodes and adult leaves at high nodes, whereas miR156 overexpressors had juvenile leaves at all nodes. The traits that showed a leaf position effect, independent of developmental phase, were $A_{\text{sat Area}}$ and $A_{\text{low light Mass}}$ in *Z. mays* and J_{max} in *P. tremula* × *alba* (Table S3).

Photosynthetic traits in *Populus tremula* × *alba* grown from seed

The analyses of *P. tremula* × *alba* already described herein were conducted with cuttings of the 717-1B4 clone propagated *in vitro.* We considered the first-formed leaves on these plants to be juvenile leaves because they differed morphologically from later-formed leaves, and because the leaves of transgenic plants overexpressing miR156 closely resembled these first-formed leaves. To determine how closely these plants resemble normal *P. tremula* × *alba*, we examined a variety of traits in successive leaves of plants grown from seeds. Consistent with the results obtained with plants propagated *in vitro*, SLA, $A_{\text{sat Area}}$, $A_{\text{low light Area}}$ and F_v/F_m all showed significant differences between juvenile and adult leaves (Table 2). All other gas-exchange and fluorescence traits did not display phase-specific differences, consistent with the results we obtained with 717-1B4 plants. These results demonstrate that photosynthetic physiology associated with VPC in *P. tremula* × *alba* plants regenerated *in vitro* is similar, if not identical, to VPC in seed-derived plants.

Discussion

Numerous studies have shown that leaves produced at different times in plant development often have different rates of photosynthesis (Bond, 2000). Here, we investigated whether this phenomenon can be attributed to the transition between juvenile and adult phases of vegetative development, a process called VPC. Previous studies have described differences in photosynthetic efficiency between juvenile and adult leaves of strongly heteroblastic species of *Eucalyptus* (Cameron, 1970; Velikova et al., 2008) and *Acacia* (Brodribb & Hill, 1993; Hansen, 1996; Yu & Li, 2007). However, it is difficult to know if these studies are generally relevant because of the large anatomical differences between juvenile and adult leaves in these species, and because these studies did not control for the effect of leaf position.

We characterized how VPC impacts photosynthesis independent of other confounding factors by manipulating the expression of miR156, the master regulator of this process. The miR156 overexpressors used in this study delay VPC, causing the plants to produce leaves with juvenile identity at positions that are normally adult. This made it possible to distinguish miR156-regulated photosynthetic traits from photosynthetic traits that vary as a function of leaf position or plant age.

In all three of the species we examined (*P. tremula* × *alba, A. thaliana* and *Z. mays*) the rate of light-saturated photosynthesis was phase dependent, although this relationship differed between species depending on whether area or mass-based measures were used (Fig. 2). Previous studies have revealed significant differences in the expression of photosynthetic genes in juvenile and adult leaves of *Z. mays* (Strable et al., 2008; Beydler, 2014) and *Malus domestica* Borkh. (Gao et al., 2014), suggesting that phase-dependent variation in the rate of photosynthesis might be attributable to differences in the biochemistry of photosynthesis in different leaves. However, multiple measures of photosynthetic capacity and light-use efficiency provided no evidence of this. Instead, we found that the difference in the rate of photosynthesis in juvenile and adult leaves was most highly correlated with differences in the SLA and N content of these leaves (Fig. 5). This observation suggests that phase-dependent differences in photosynthetic rates are attributable to differences in leaf anatomy and leaf composition, rather than differences in the biochemistry of photosynthesis.

Leaf morphology and composition have robust relationships with photosynthesis across species and environments (Niinemets & Tenhunen, 1997; Reich et al., 1998, 1999, 2003; Meziane & Shipley, 2001). Leaf thickness and tissue density – the structural changes that determine SLA – modulate intra-leaf light dynamics, CO_2 diffusion, and the distribution of leaf N (Parkhurst, 1994; Epron et al., 1995; Terashima & Hikosaka, 1995; Reich et al., 1998; Terashima et al., 2006; Evans et al., 2009). Specifically, variation in SLA changes the way light moves within the leaf, as path length and scattering are altered. This leads to leaves with low SLA absorbing more light per area as path length increases, ultimately leading to higher $A_{\text{sat Area}}$ (Terashima & Hikosaka, 1995). However, leaves with low SLA face the challenge of increased CO_2 diffusion resistance, as CO_2 must travel farther from stomata and through denser tissue to reach carboxylating enzymes (Parkhurst, 1994; Terashima et al., 2006). SLA further impacts photosynthesis through the distribution of leaf N, as leaves with low SLA are associated with more cytoplasmic volume per leaf area, and therefore more N. The relationship between leaf N and photosynthesis results from the well-established relationship between N, Rubisco, and other photosynthetically important proteins (Field & Mooney, 1986; Evans, 1989; Ellsworth & Reich, 1993; Makino et al., 1994; Bond et al., 1999; Chmura & Tjoelker, 2008). These mechanisms describe how the physical properties of a leaf can alter photosynthetic rates independent of changes in biochemistry, supporting what we found in the developmentally distinct leaves of three species.

It is currently unclear why phase dependence in A_{sat} and leaf N are observed in area-based measures for *P. tremula* × *alba* and *A. thaliana* but in mass-based measures for *Z. mays* (although the fact that only one form of measurement correlates with SLA and leaf N is expected) (Westoby et al., 2013). These three species all have relatively high SLA, and no differences in PNUE between juvenile and adult leaves (Table 1), which would suggest differences in the A_{sat}–N slope due to SLA (Reich et al., 1998) do not contribute to this phenomenon. Other potential explanations include differences in photosynthetic pathway (C_3 vs C_4), developmental form (dicot vs monocot), or variation in the morphological contributors to SLA (leaf thickness vs cell density). Because the relationships between SLA and photosynthetic rate are conserved across data sets that include both C_3 and C_4 species as well as both monocots and dicots, these traits are unlikely to explain the differences between species in this study (Reich et al., 1999, 2003; Meziane & Shipley, 2001). Though density

and thickness each contribute to variation in SLA, the degree to which they alter the photosynthetically important properties of a leaf vary. Because of this, Niinemets (1999) found that changes in leaf thickness are more closely correlated with area-based photosynthetic rates and changes in density are correlated with mass-based rates. As to be expected, changes in both leaf thickness and density have been associated with changes in SLA across all three study species (Bongard-Pierce et al., 1996; Chuck et al., 2011; Wang et al., 2011; Coneva & Chitwood, 2018) and can be observed in cross-sections of adult, juvenile, and juvenilized leaves in this study (Fig. 4). Further studies are needed to determine the extent to which density and thickness contribute to phase-dependent changes in SLA and the mass or area-based correlations observed in this study.

Juvenile leaf morphology and photosynthetic properties may contribute to better survival in low-light environments, such as those frequently experienced by juvenile tissues at the bottom of a canopy. High SLA, found in juvenile leaves of all three species, is strongly correlated with higher photosynthetic rates under light-limited conditions and shade tolerance (Givnish, 1988; Niinemets & Tenhunen, 1997; Walters & Reich, 1999; Reich et al., 2003). In support of this hypothesis, the juvenile leaves in each species had higher mass-based photosynthetic rates at low light levels ($A_{\text{low light Mass}}$) than adult leaves did (Fig. 7d–f; Table 3). Even in area-based measures of *P. tremula* × *alba* and *A. thaliana*, where adult leaves have higher A_{sat}, this photosynthetic advantage is lost under light-limited conditions (Fig. 7a–c). Further, variation in photosynthesis and SLA have been associated with tolerance to additional environmental factors, including drought and herbivory, and with changes in growth strategy, such as leaf life-span and growth rate (Poorter, 1999; Wright & Cannon, 2001; Reich et al., 2003; Poorter et al., 2009; Niinemets, 2010; Dayrell et al., 2018). Because these traits are phase dependent, it is likely that, during a plant's lifetime, VPC contributes to variation in biotic and abiotic stress tolerance through changes in leaf morphology and photosynthesis, in addition to previously identified mechanisms (Stief et al., 2014; Cui et al., 2014; Arshad et al., 2017; Ge et al., 2018; Leichty & Poethig, 2019; Visentin et al., 2020).

Our observation that SLA and the rate of photosynthesis change in a coordinated and phase-dependent fashion in three phylogenetically diverse species suggests that the phase dependence of these traits is widespread in flowering plants. The observation that these traits are independent of plant size and age also suggests that natural selection on the rate of photosynthesis may play an important role in the morphological adaptation of plants to their environment. In particular, conditions that favor juvenile or adult patterns of photosynthesis could drive changes in the timing of VPC, which would in turn lead to changes in numerous other phase-dependent vegetative traits. Determining how photosynthesis and other phase-dependent processes interact to influence plant performance is crucial for understanding plant ecology and evolution.

Supplementary Material

Refer to Web version on PubMed Central for supplementary material.

Acknowledgements

We thank Samara Gray and Joshua Darfler for their assistance in caring for the plants used in this study and Che-Ling Ho for assistance with leaf cross-sections. This research was funded by the NSF Graduate Research Fellowship (Division of Graduate Education; DGE-1845298), University of Pennsylvania SAS Dissertation Research Fellowship and the Peachey Research Fund awarded to EHL, and NIH GM51893 awarded to RSP.

References

Ahsan MU, Hayward A, Alam M, Bandaralage JH, Topp B, Beveridge CA, Mitter N. 2019. Scion control of miRNA abundance and tree maturity in grafted avocado. BMC Plant Biology 19: e382.

Arshad M, Feyissa BA, Amyot L, Aung B, Hannoufa A. 2017. MicroRNA156 improves drought stress tolerance in alfalfa (*Medicago sativa*) by silencing SPL13. Plant Science 258: 122–136. [PubMed: 28330556]

Axtell MJ, Bowman JL. 2008. Evolution of plant microRNAs and their targets. Trends in Plant Science 13: 343–349. [PubMed: 18502167]

Bassiri A, Irish EE, Scott PR. 1992. Heterochronic effects of *Teopod 2* on the growth and photosensitivity of the maize shoot. Plant Cell 4: 497–504. [PubMed: 12297653]

Bauer H, Bauer U. 1980. Photosynthesis in leaves of the juvenile and adult phase of ivy (*Hedera helix*). Physiologia Plantarum 49: 366–372.

Beydler BD. 2014. Dynamics of gene expression during vegetative phase change in dynamics of gene expression during vegetative phase change in maize. PhD thesis, University of Iowa, Iowa City, IA, USA.

Bhogale S, Mahajan AS, Natarajan B, Rajabhoj M, Thulasiram HV, Banerjee AK. 2014. *MicroRNA156*: a potential graft-transmissible microRNA that modulates plant architecture and tuberization in *Solanum tuberosum* ssp. *andigena*. Plant Physiology 164: 1011–1027. [PubMed: 24351688]

Bond BJ. 2000. Age-related changes in photosynthesis of woody plants. Trends in Plant Science 5: 349–353. [PubMed: 10908880]

Bond BJ, Farnsworth BT, Coulombe RA, Winner WE. 1999. Foliage physiology and biochemistry in response to light gradients in conifers with varying shade tolerance. Oecologia 120: 183–192. [PubMed: 28308078]

Bongard-Pierce DK, Evans MMS, Poethig RS. 1996. Heteroblastic features of leaf anatomy in maize and their genetic regulation. International Journal of Plant Sciences 157: 331.

Brodribb T, Hill RS. 1993. A physiological comparison of leaves and phyllodes in *Acacia melanoxylon*. Australian Journal of Botany 41: 293–305.

Cameron RJ. 1970. Light intensity and the growth of *Eucalyptus* seedlings. I. Ontogenetic variation in *E. fastigata*. Australian Journal of Botany 18: 29–43.

Canham CD. 1988. An index for understory light levels in and around canopy gaps. Ecology 69: 1634–1638.

Canham CD, Finzi AC, Pacala SW, Burbank DH. 1994. Causes and consequences of resource heterogeneity in forests: interspecific variation in light transmission by canopy trees. Canadian Journal of Forest Research 24: 337–349.

Cavender-Bares J, Bazzaz FA. 2000. Changes in drought response strategies with ontogeny in *Quercus rubra*: implications for scaling from seedlings to mature trees. Oecologia 124: 8–18. [PubMed: 28308415]

Charles LS, Dwyer JM, Smith TJ, Connors S, Marschner P, Mayfield MM. 2018. Seedling growth responses to species, neighborhood, and landscape-scale effects during tropical forest restoration. Ecosphere 9: e02386.

Chmura DJ, Tjoelker MG. 2008. Leaf traits in relation to crown development, light interception and growth of elite families of loblolly and slash pine. Tree Physiology 28: 729–742. [PubMed: 18316305]

Chuck G, Cigan M, Saeteurn K, Hake S. 2007. The heterochronic maize mutant *Corngrass1* results from overexpression of a tandem microRNA. Nature Genetics 39: 544–549. [PubMed: 17369828]

Chuck GS, Tobias C, Sun L, Kraemer F, Li C, Dibble D, Arora R, Bragg JN, Vogel JP, Singh S et al. 2011. Overexpression of the maize *Corngrass1* microRNA prevents flowering, improves digestibility, and increases starch content of switchgrass. Proceedings of the National Academy of Sciences, USA 109: 995.

Coneva V, Chitwood DH. 2018. Genetic and developmental basis for increased leaf thickness in the Arabidopsis Cvi ecotype. Frontiers in Plant Science 9: e322.

Cui L-G, Shan J-X, Shi M, Gao J-P, Lin H-X. 2014. The *miR156-SPL9-DFR* pathway coordinates the relationship between development and abiotic stress tolerance in plants. The Plant Journal 80: 1108–1117. [PubMed: 25345491]

Dayrell RLC, Arruda AJ, Pierce S, Negreiros D, Meyer PB, Lambers H, Silveira FAO. 2018. Ontogenetic shifts in plant ecological strategies. Functional Ecology 32: 2730–2741.

de Lobo FA, de Barros MP, Dalmagro HJ, Dalmolin ÂC, Pereira WE, de Souza ÉC, Vourlitis GL, Rodríguez Ortíz CE 2013. Fitting net photosynthetic light-response curves with Microsoft EXCEL – a critical look at the models. Photosynthetica 51: 445–456.

Duursma RA. 2015. PLANTECOPHYS – an R package for analysing and modelling leaf gas exchange data. PLoS ONE 10: e0143346. [PubMed: 26581080]

Ellsworth DS, Reich PB. 1993. Canopy structure and vertical patterns of photosynthesis and related leaf traits in a deciduous forest. Oecologia 96: 169–178. [PubMed: 28313412]

Epron D, Godard D, Cornic G, Genty B. 1995. Limitation of net CO_2 assimilation rate by internal resistances to CO_2 transfer in the leaves of two tree species (*Fagus sylvatica* L. and *Castanea sativa* Mill.). Plant, Cell & Environment 18: 43–51.

Evans GC, Coombe DE. 1959. Hemispherical and woodland canopy photography and the light climate. The Journal of Ecology 47: 103–113.

Evans JR. 1989. Photosynthesis and nitrogen relationships in leaves of C_3 plants. Oecologia 78: 9–19. [PubMed: 28311896]

Evans JR, Kaldenhoff R, Genty B, Terashima I. 2009. Resistances along the CO_2 diffusion pathway inside leaves. Journal of Experimental Botany 60: 2235–2248. [PubMed: 19395390]

Feng S, Xu Y, Guo C, Zheng J, Zhou B, Zhang Y, Ding Y, Zhang L, Zhu Z, Wang H et al. 2016. Modulation of miR156 to identify traits associated with vegetative phase change in tobacco (*Nicotiana tabacum*). Journal of Experimental Botany 67: 1493–1504. [PubMed: 26763975]

Field C, Mooney HA. 1986. The photosynthesis–nitrogen relationship in wild plants. In: Givnish TJ, ed. On the economy of plant form and function. Cambridge, UK: Cambridge University Press, 25–55.

Flexas J, Ortuño MF, Ribas-Carbo M, Diaz-Espejo A, Flórez-Sarasa ID, Medrano H. 2007. Mesophyll conductance to CO_2 in *Arabidopsis thaliana*. New Phytologist 175: 501–511.

Fouracre JP, Poethig RS. 2019. Role for the shoot apical meristem in the specification of juvenile leaf identity in *Arabidopsis*. Proceedings of the National Academy of Sciences, USA 116: 10168–10177.

Gao Y, Yang FQ, Cao X, Li CM, Wang Y, Zhao YB, Zeng GJ, Chen DM, Han ZH, Zhang XZ. 2014. Differences in gene expression and regulation during ontogenetic phase change in apple seedlings. Plant Molecular Biology Reporter 32:357–371.

Ge Y, Han J, Zhou G, Xu Y, Ding Y, Shi M, Guo C, Wu G. 2018. Silencing of miR156 confers enhanced resistance to brown planthopper in rice. Planta 248: 813–826. [PubMed: 29934776]

Givnish TJ. 1988. Adaptation to sun and shade: a whole-plant perspective. Australian Journal of Plant Physiology 15: 63–92.

Grossnickle SC. 2012. Why seedlings survive: influence of plant attributes. New Forests 43: 711–738.

Hahn PG, Orrock JL. 2016. Neighbor palatability generates associational effects by altering herbivore foraging behavior. Ecology 97: 2103–2111. [PubMed: 27859184]

Hansen DH. 1996. Establishment and persistence characteristics in juvenile leaves and phyllodes of *Acacia koa* (Leguminosae) in Hawaii. International Journal of Plant Sciences 157: 123–128.

He J, Xu M, Willmann MR, McCormick K, Hu T, Yang L, Starker CG, Voytas DF, Meyers BC, Poethig RS. 2018. Threshold-dependent repression of *SPL* gene expression by miR156/miR157 controls vegetative phase change in *Arabidopsis thaliana*. PLoS Genetics 14: e1007337. [PubMed: 29672610]

Huang L-C, Weng J-H, Wang C-H, Kuo C-I, Shieh Y-J. 2003. Photosynthetic potentials of *in vitro*-grown juvenile, adult, and rejuvenated *Sequoia sempervirens* (D. Don) Endl. shoots. Botanical Bulletin of Academia Sinica 44: 31–35.

Hutchison KW, Sherman CD, Weber J, Smith SS, Singer PB, Greenwood MS. 1990. Maturation in larch: II. Effects of age on photosynthesis and gene expression in developing foliage. Plant Physiology 94: 1308–1315. [PubMed: 16667834]

Irish EE, Karlen S. 1998. Restoration of juvenility in maize shoots by meristem culture. International Journal of Plant Sciences 159: 695–701.

Ishida A, Yazaki K, Hoe AL. 2005. Ontogenetic transition of leaf physiology and anatomy from seedlings to mature trees of a rain forest pioneer tree, *Macaranga gigantea*. Tree Physiology 25: 513–522. [PubMed: 15741149]

Jaya E, Kubien DS, Jameson PE, Clemens J. 2010. Vegetative phase change and photosynthesis in *Eucalyptus occidentals:* architectural simplification prolongs juvenile traits. Tree Physiology 30: 393–403. [PubMed: 20100699]

Kabrick JM, Knapp BO, Dey DC, Larsen DR. 2015. Effect of initial seedling size, understory competition, and overstory density on the survival and growth of *Pinus echinata* seedlings underplanted in hardwood forests for restoration. New Forests 46: 897–918.

Kerr KL, Meinzer FC, McCulloh KA, Woodruff DR, Marias DE. 2015. Expression of functional traits during seedling establishment in two populations of *Pinus ponderosa* from contrasting climates. Tree Physiology 35: 535–548. [PubMed: 25934987]

Kitajima K, Cordero RA, Wright SJ. 2013. Leaf life span spectrum of tropical woody seedlings: effects of light and ontogeny and consequences for survival. Annals of Botany 112: 685–699. [PubMed: 23532047]

Kubien D, Jaya E, Clemens J. 2007. Differences in the structure and gas exchange physiology of juvenile and adult leaves in *Metrosideros excelsa*. International Journal of Plant Sciences 168: 563–570.

Kuusk V, Niinemets Ü, Valladares F. 2018a. A major trade-off between structural and photosynthetic investments operative across plant and needle ages in three Mediterranean pines. Tree Physiology 38: 543–557. [PubMed: 29281105]

Kuusk V, Niinemets Ü, Valladares F. 2018b. Structural controls on photosynthetic capacity through juvenile-to-adult transition and needle ageing in Mediterranean pines. Functional Ecology 32: 1479–1491.

Lamb EG, Cahill JF. 2006. Consequences of differing competitive abilities between juvenile and adult plants. Oikos 112: 502–512.

Lasky JR, Bachelot B, Muscarella R, Schwartz N, Forero-Montaña J, Nytch CJ, Swenson NG, Thompson J, Zimmerman JK, Uriarte M. 2015. Ontogenetic shifts in trait-mediated mechanisms of plant community assembly. Ecology 96: 2157–2169. [PubMed: 26405741]

Lawrence EH, Leichty AR, Ma C, Strauss SH, Poethig RS. 2020. Vegetative phase change in *Populus tremula* × *alba*. bioRxiv: 2020.06.21.163469.

Lawrence EH, Stinziano JR, Hanson DT. 2019. Using the rapid A–C_i response (RACiR) in the Li-Cor 6400 to measure developmental gradients of photosynthetic capacity in poplar. Plant Cell and Environment 42: 740–750.

Leichty AR, Poethig RS. 2019. Development and evolution of age-dependent defenses in ant-acacias. Proceedings of the National Academy of Sciences, USA 116: 15596–15601.

Li H, Zhao X, Dai H, Wu W, Mao W, Zhang Z. 2012. Tissue culture responsive microRNAs in strawberry. Plant Molecular Biology Reporter 30: 1047–1054.

Lusk CH, Del Pozo A. 2002. Survival and growth of seedlings of 12 Chilean rainforest trees in two light environments: gas exchange and biomass distribution correlates. Austral Ecology 27: 173–182.

Makino A, Nakano H,Mae T. 1994. Responses of ribulose-1,5-bisphosphate carboxylase, cytochrome *f*, and sucrose synthesis enzymes in rice leaves to leaf nitrogen and their relationships to photosynthesis. Plant Physiology 105: 173–179. [PubMed: 12232197]

Marin-Gonzalez E, Suarez-Lopez P. 2012. 'And yet it moves': cell-to-cell and long-distance signaling by plant microRNAs. Plant Science 196: 18–30. [PubMed: 23017896]

Meilan R, Ma C. 2006. Poplar (*Populus* spp.). In: Wang K, ed. Methods in molecular biology: agrobacterium protocols. Totowa, NJ, USA: Humana Press Inc., 143–151.

Meziane D, Shipley B. 2001. Direct and indirect relationships between specific leaf area, leaf nitrogen and leaf gas exchange. Effects of irradiance and nutrient supply. Annals of Botany 88: 915–927.

Modrzynski J, Chmura DJ, Tjoelker MG. 2015. Seedling growth and biomass allocation in relation to leaf habit and shade tolerance among 10 temperate tree species. Tree Physiology 35: 879–893. [PubMed: 26116924]

Moll JD, Brown JS. 2008. Competition and coexistence with multiple life-history stages. The American Naturalist 171: 839–843.

Niinemets Ü 1999. Components of leaf dry mass per area – thickness and density – alter leaf photosynthetic capacity in reverse directions in woody plants. New Phytologist 144: 35–47.

Niinemets Ü 2010. Responses of forest trees to single and multiple environmental stresses from seedlings to mature plants: past stress history, stress interactions, tolerance and acclimation. Forest Ecology and Management 260: 1623–1639.

Niinemets Ü, Tenhunen JD. 1997. A model separating leaf structural and physiological effects on carbon gain along light gradients for the shade-tolerant species *Acer saccharum*. Plant, Cell & Environment20: 845–866.

Parish JAD, Bazzaz FA. 1985. Ontogenetic niche shifts in old-field annuals. Ecology 66: 1296–1302.

Parkhurst DF. 1994. Diffusion of CO_2 and other gases inside leaves. New Phytologist 126: 449–479.

Piao T, Comita LS, Jin G, Kim JH. 2013. Density dependence across multiple life stages in a temperate old-growth forest of northeast China. Oecologia 172: 207–217. [PubMed: 23053238]

Poethig RS. 1988. Heterochronic mutations affecting shoot development in maize. Genetics 119: 959–973. [PubMed: 17246439]

Poethig RS. 1990. Phase change and the regulation of shoot morphogenesis in plants. Science 250: 923–930. [PubMed: 17746915]

Poorter H, Niinemets Ü, Poorter L, Wright IJ, Villar R. 2009. Causes and consequences of variation in leaf mass per area (LMA): a meta-analysis. New Phytologist 182: 565–588.

Poorter L 1999. Growth responses of 15 rain-forest tree species to a light gradient: the relative importance of morphological and physiological traits. Functional Ecology 13: 396–410.

Poorter L, Bongers F. 2006. Leaf traits are good predictors of plant performance across 53 rain forest species. Ecology 87: 1733–1743. [PubMed: 16922323]

Porra RJ, Thompson WA, Kriedemann PE. 1989. Determination of accurate extinction coefficients and simultaneous equations for assaying chlorophylls *a* and *b* extracted with four different solvents: verification of the concentration of chlorophyll standards by atomic absorption spectroscopy. Biochimica et Biophysica Acta 975: 384–394.

Reich PB, Ellsworth DS, Walters MB. 1998. Leaf structure (specific leaf area) modulates photosynthesis–nitrogen relations: evidence from within and across species and functional groups. Functional Ecology 12: 948–958.

Reich PB, Ellsworth DS, Walters MB, Vose JM, Gresham C, Volin JC, Bowman WD. 1999. Generality of leaf trait relationships: a test across six biomes. Ecology 80: 1955–1969.

Reich PB, Wright IJ, Cavender-Bares J, Craine JM, Oleksyn J, Westoby M, Walters MB. 2003. The evolution of plant functional variation: traits, spectra, and strategies. International Journal of Plant Sciences 164: S143–S164.

Shuttleworth WJ, Gash JHC, Lloyd CR, Moore CJ, Roberts J, de Marques Filho AO, Fisch G, de Silva Filho VP, de Nazare Goes Ribeiro M, Molion LCB et al. 1985. Daily variations of temperature and humidity within and above Amazonian forest. Weather 40: 102–108.

Silva PO, Batista DS, Henrique J, Cavalcanti F, Koehler AD, Vieira LM, Fernandes AM, Hernan Barrera-Rojas C, Ribeiro DM, Nogueira FTS et al. 2019. Leaf heteroblasty in *Passiflora edulis* as revealed by metabolic profiling and expression analyses of the microRNAs miR156 and miR172. Annals of Botany 123: 1191–1203. [PubMed: 30861065]

Spasojevic MJ, Yablon EA, Oberle B, Myers JA. 2014. Ontogenetic trait variation influences tree community assembly across environmental gradients. Ecosphere 5: 1–20.

Steppe K, Niinemets Ü, Teskey RO. 2011. Tree size and age-related changes in leaf physiology and their influence on carbon gain. In: Meinzer FC, Lachenbruch B, Dawson TE, eds. Size and age-related changes in tree structure and function. New York, NY, USA: Springer, 235–253.

Stief A, Altmann S, Hoffmann K, Pant BD, Scheible W-R, Bäurle I. 2014. *Arabidopsis miR156* regulates tolerance to recurring environmental stress through *SPL* transcription factors. Plant Cell 26: 1792–1807. [PubMed: 24769482]

Still C, Powell R, Aubrecht D, Kim Y, Helliker B, Roberts D, Richardson AD, Goulden M. 2019. Thermal imaging in plant and ecosystem ecology: applications and challenges. Ecosphere 10: e02768.

Strable J, Borsuk L, Nettleton D, Schnable PS, Irish EE. 2008. Microarray analysis of vegetative phase change in maize. The Plant Journal 56: 1045–1057. [PubMed: 18764925]

Sun J, Yao F, Wu J, Zhang P, Xu W. 2018. Effect of nitrogen levels on photosynthetic parameters, morphological and chemical characters of saplings and trees in a temperate forest. Journal of Forestry Research 29: 1481–1488.

Telfer A, Bollman KM, Poethig RS. 1997. Phase change and the regulation of trichome distribution in *Arabidopsis thaliana*. Development 124: 645–654. [PubMed: 9043079]

Terashima I, Hanba YT, Tazoe Y, Vyas P, Yano S. 2006. Irradiance and phenotype: comparative eco-development of sun and shade leaves in relation to photosynthetic CO_2 diffusion. Journal of Experimental Botany. 57: 343–354. [PubMed: 16356943]

Terashima I, Hikosaka K. 1995. Comparative ecophysiology of leaf and canopy photosynthesis. Plant, Cell & Environment 18: 1111–1128.

Tomeo N 2019. Tomeopaste/AQ_curves: AQ_curve fitting release 1 (v.1.0.0). Zenodo. doi: 10.5281/zenodo.3497557.

Velikova V, Loreto F, Brilli F, Stefanov D, Yordanov I. 2008. Characterization of juvenile and adult leaves of *Eucalyptus globulus* showing distinct heteroblastic development: photosynthesis and volatile isoprenoids. Plant Biology 10: 55–64. [PubMed: 18211547]

Visentin I, Pagliarani C, Deva E, Caracci A, Turečková V, Novák O, Lovisolo C, Schubert A, Cardinale F. 2020. A novel strigolactone-miR156 module controls stomatal behaviour during drought recovery. Plant, Cell & Environment 43: 1613–1624.

Waggoner PE, Reifsnyder WE. 1968. Simulation of the temperature, humidity and evaporation profiles in a leaf canopy. Journal of Applied Meteorology 7: 400–409.

Walters MB, Reich PB. 1999. Low-light carbon balance and shade tolerance in the seedlings of woody plants: do winter deciduous and broad-leaved evergreen species differ? New Phytologist 143: 143–154.

Wang JW, Park MY, Wang LJ, Koo Y, Chen XY, Weigel D, Poethig RS.2011. MiRNA control of vegetative phase change in trees. PLoS Genetics 7: e1002012. [PubMed: 21383862]

Westoby M, Reich PB, Wright IJ. 2013. Understanding[tsl] ecological variation across species: area-basedvs mass-based expression of leaf traits. New Phytologist 199: 322–323.

Willmann MR., Poethig RS. 2007. Conservation and evolution of miRNA regulatory programs in plant development. Current Opinion in Plant Biology 10: 503–511. [PubMed: 17709279]

Wright IJ, Cannon K. 2001. Relationships between leaf lifespan and structural defences in a low-nutrient, sclerophyll flora. Functional Ecology 15: 351–359.

Wu G, Park MY, Conway SR, Wang JW, Weigel D, Poethig RS. 2009. The sequential action of miR156 and miR172 regulates developmental timing in *Arabidopsis*. Cell 138: 750–759. [PubMed: 19703400]

Wu G, Poethig RS. 2006. Temporal regulation[tsl] of shoot development in *Arabidopsis thaliana by miR156* and its target *SPL3*. Development 133: 3539–3547. [PubMed: 16914499]

Xu M, Hu T, Zhao J, Park M-Y, Earley KW, Wu G, Yang L, Poethig RS. 2016. Developmental functions of miR156-regulated *SQUAMOSA PROMOTER BINDING PROTEIN-LIKE* (*SPL*) genes in *Arabidopsis thaliana*. PLoS Genetics 12: e1006263. [PubMed: 27541584]

Yin X, Sun Z, Struik PC, Van Der Putten PEL, Van Ieperen W, Harbinson J. 2011. Using a biochemical C_4 photosynthesis model and combined gas exchange and chlorophyll fluorescence measurements to estimate bundle-sheath conductance of maize leaves differing in age and nitrogen content. Plant, Cell & Environment 34: 2183–2199.

Yu H, Li JT. 2007. Physiological comparisons of true leaves and phyllodes in Acacia mangium seedlings. Photosynthetica 45: 312–316.

Zhang SD, Ling LZ, Zhang QF, Di XuJ, Cheng L. 2015. Evolutionary comparison of two combinatorial regulators of SBP-box genes, *MiR156* and *MiR529*, in plants. PLoS ONE 10: e0124621. [PubMed: 25909360]

Zhou H, Akây E, Helliker BR. 2019. Estimating C_4 photosynthesis parameters by fitting intensive A/C_i curves. Photosynthesis Research 141: 181–194. [PubMed: 30758752]

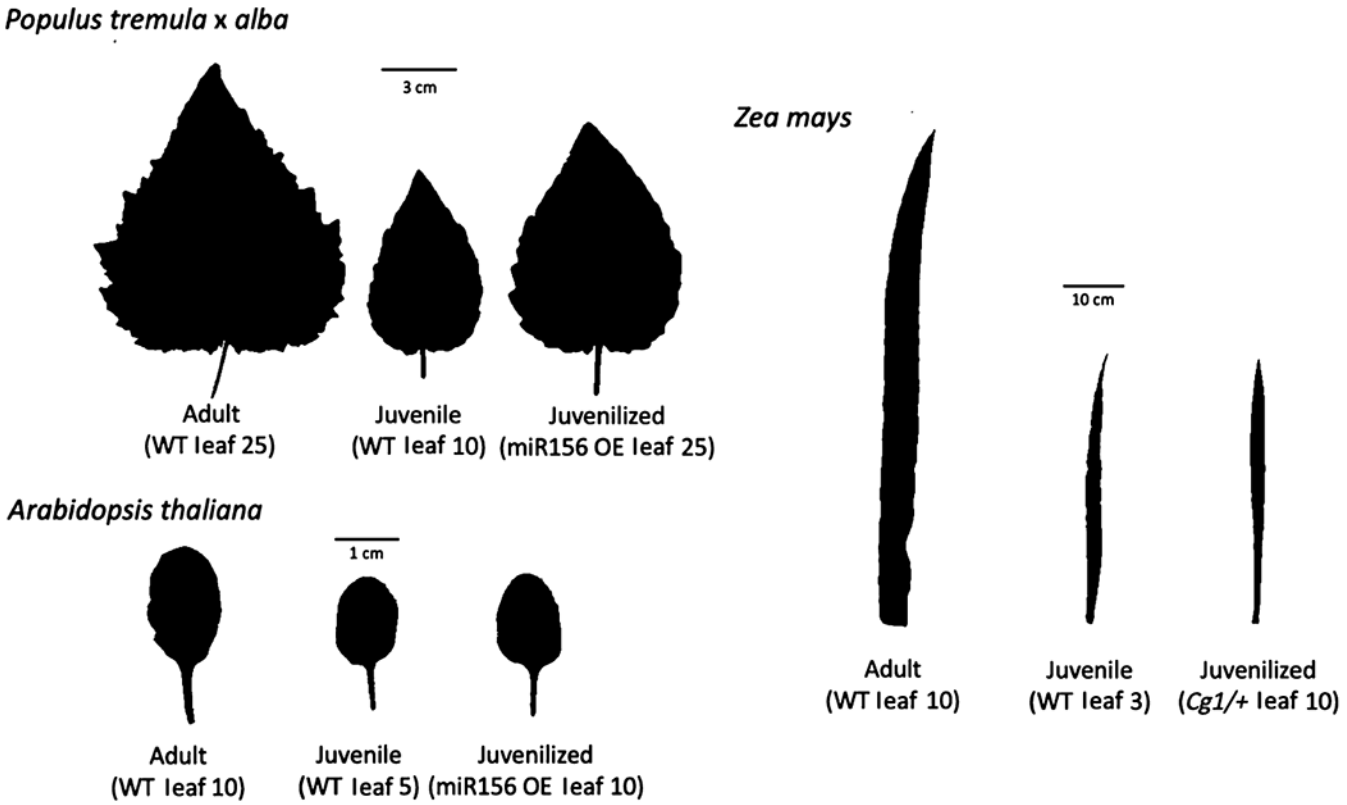

Fig. 1.

Leaf shape phenotypes of fully expanded adult, juvenile, and juvenilized leaves of *Populus tremula* × *alba, Arabidopsis thaliana*, and *Zea mays. Cg1, Corngrass 1*; OE, overexpressor; WT, wild-type.

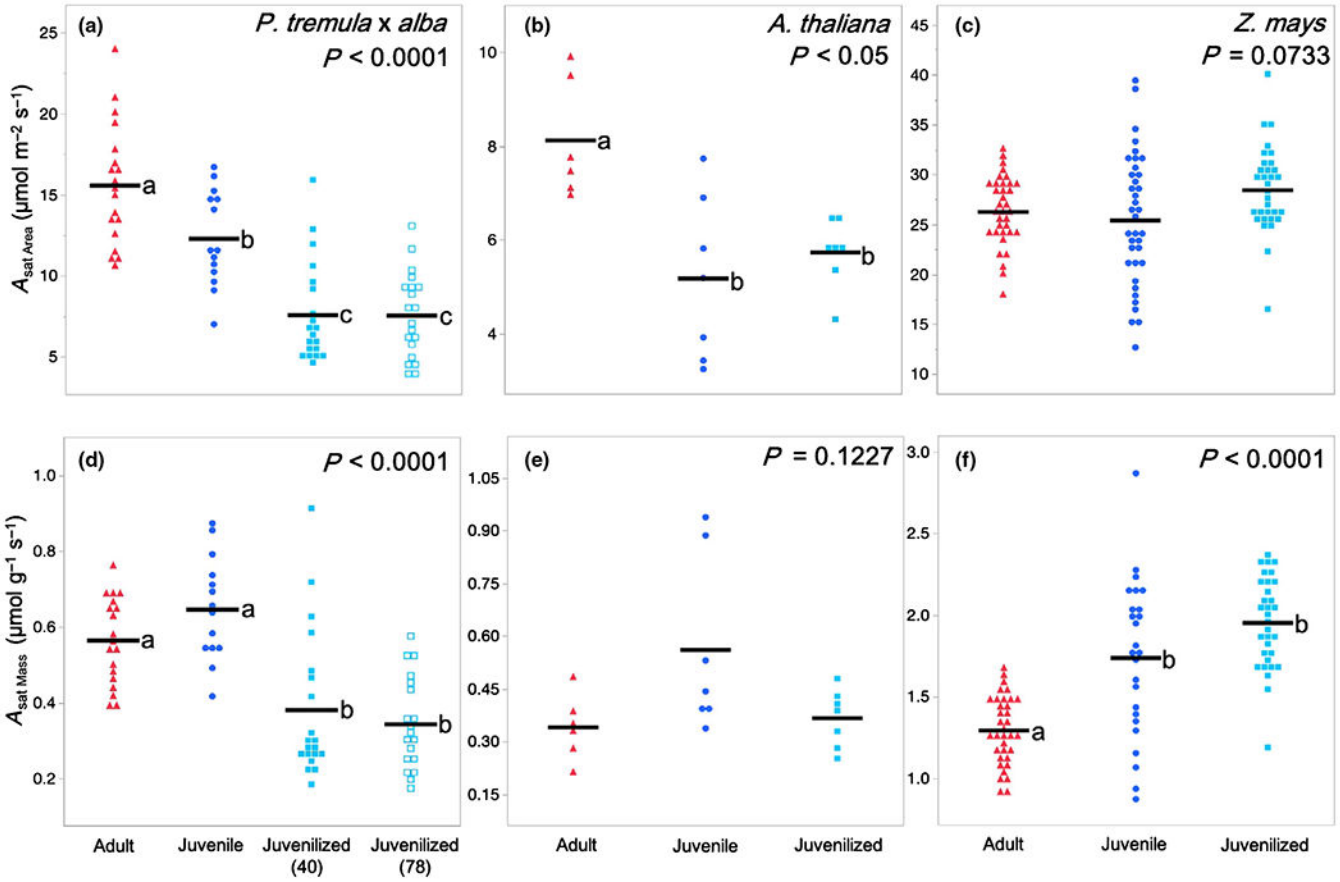

Fig. 2.

Photosynthetic rates of adult (red triangles), juvenile (blue circles), and juvenilized (light blue closed or open squares) leaves of (a, d) *Populus tremula* × *alba*, (b, e) *Arabidopsis thaliana*, and (c, f) *Zea mays*. Traits depicted are (a–c) area-based light-saturated net photosynthetic rate ($A_{\text{sat Area}}$) and (d–f) mass-based light-saturated net photosynthetic rate ($A_{\text{sat Mass}}$). Means presented as black horizontal lines. *P*-values from one-way ANOVA with development as the main effect. For traits with significant ANOVA results ($P < 0.05$), different lower-case letters indicate means of developmental stage are significantly different according to Student's *t*-test ($P < 0.05$).

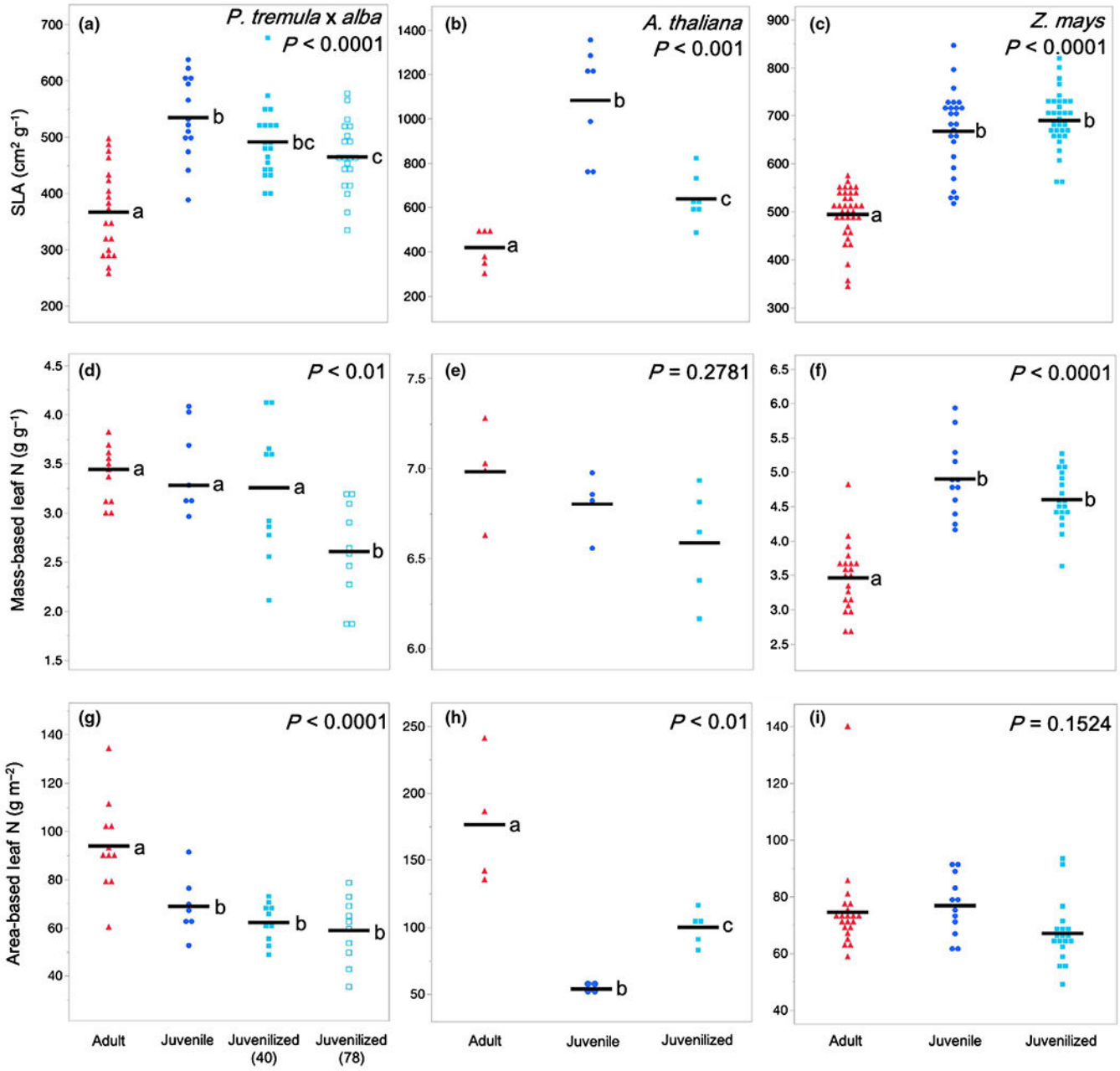

Fig. 3.

Leaf morphological and compositional traits of adult (red triangles), juvenile (blue circles), and juvenilized (light blue closed or open squares) leaves of (a, d, g) *Populus tremula* × *alba*, (b, e, h) *Arabidopsis thaliana*, and (c, f, i) *Zea mays*. Traits depicted are (a–c) specific leaf area (SLA), (d–f) mass-based leaf nitrogen (N) content, and (g–i) area-based leaf N content. Means presented as black horizontal lines. *P*-values from one-way ANOVA with development as the main effect. For traits with significant ANOVA results ($P < 0.05$) different lower-case letters indicate means of developmental stage are significantly different according to Student's *t*-test ($P < 0.05$).

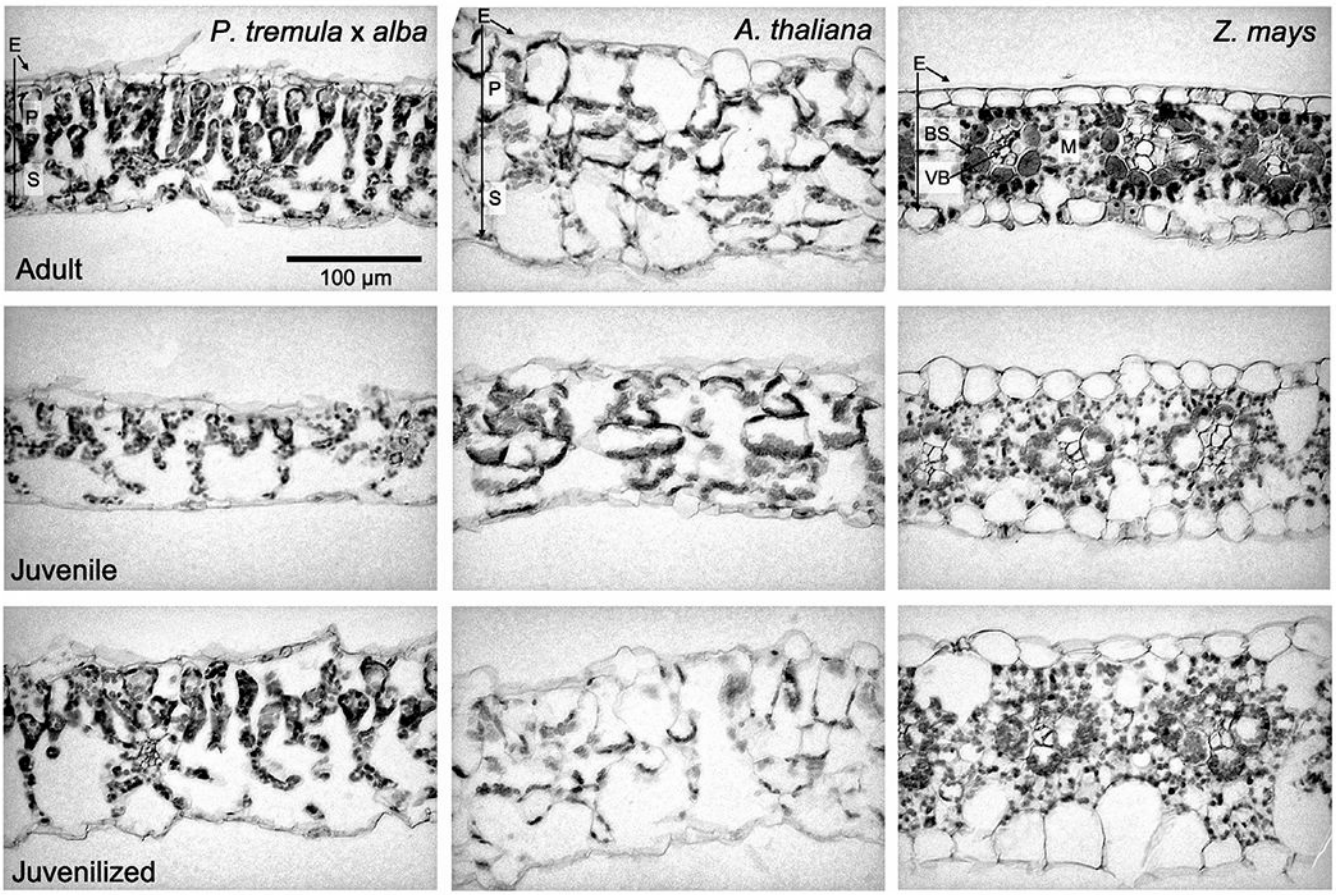

Fig. 4.

Leaf cross-sections of *Populus tremula* × *alba, Arabidopsis thaliana*, and *Zea mays* adult, juvenile, and juvenilized leaves stained with safranin-O and fast green. E, epidermis; P, palisade tissues; S, spongy tissues; BS, bundle sheath; VB, vascular bundle; M, mesophyll.

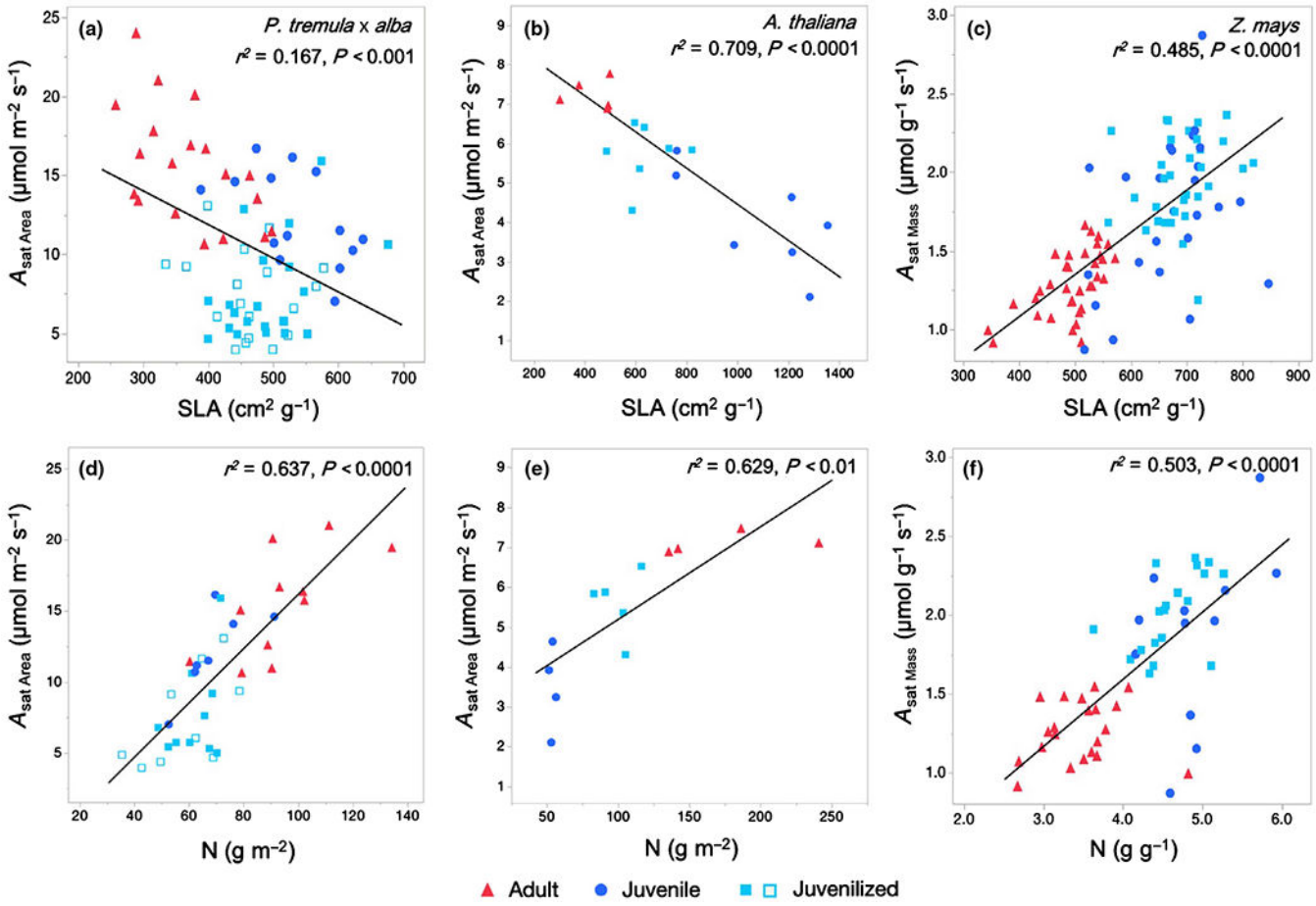

Fig. 5.

Phase-dependent light-saturated photosynthetic rates A_{sat} are significantly correlated with the leaf composition traits specific leaf area (SLA) and leaf nitrogen (N) in (a, d) *Populus tremula* × *alba*, (b, e) *Arabidopsis thaliana*, and (c, f) *Zea mays*. *Populus tremula* × *alba* and *A. thaliana* show significant differences between developmental phase in area-based measures, whereas *Z. mays* shows phase dependence in mass-based measures. Leaf developmental phase represented as adult (red triangles), juvenile (blue circles), and juvenilized (light blue closed or open squares). *P*-values and r^2 from linear regression analysis displayed in upper right corner of each panel. Linear fits for panels (a)–(f) are as follows: (a) $A_{sat\ Area} = 20.41 - 0.02134(SLA)$; (b) $A_{sat\ Area} = 9.049 - 0.004591(SLA)$; (c) $A_{sat\ Mass} = 0.01188 + 0.002678(SLA)$; (d) $A_{sat\ Area} = -2.948 + 0.1911(N_{area})$; (e) $A_{sat\ Area} = 2.867 + 0.02324\ (N_{area})$; (f) $A_{sat\ Mass} = -0.1081 + 0.4253(N_{mass})$.

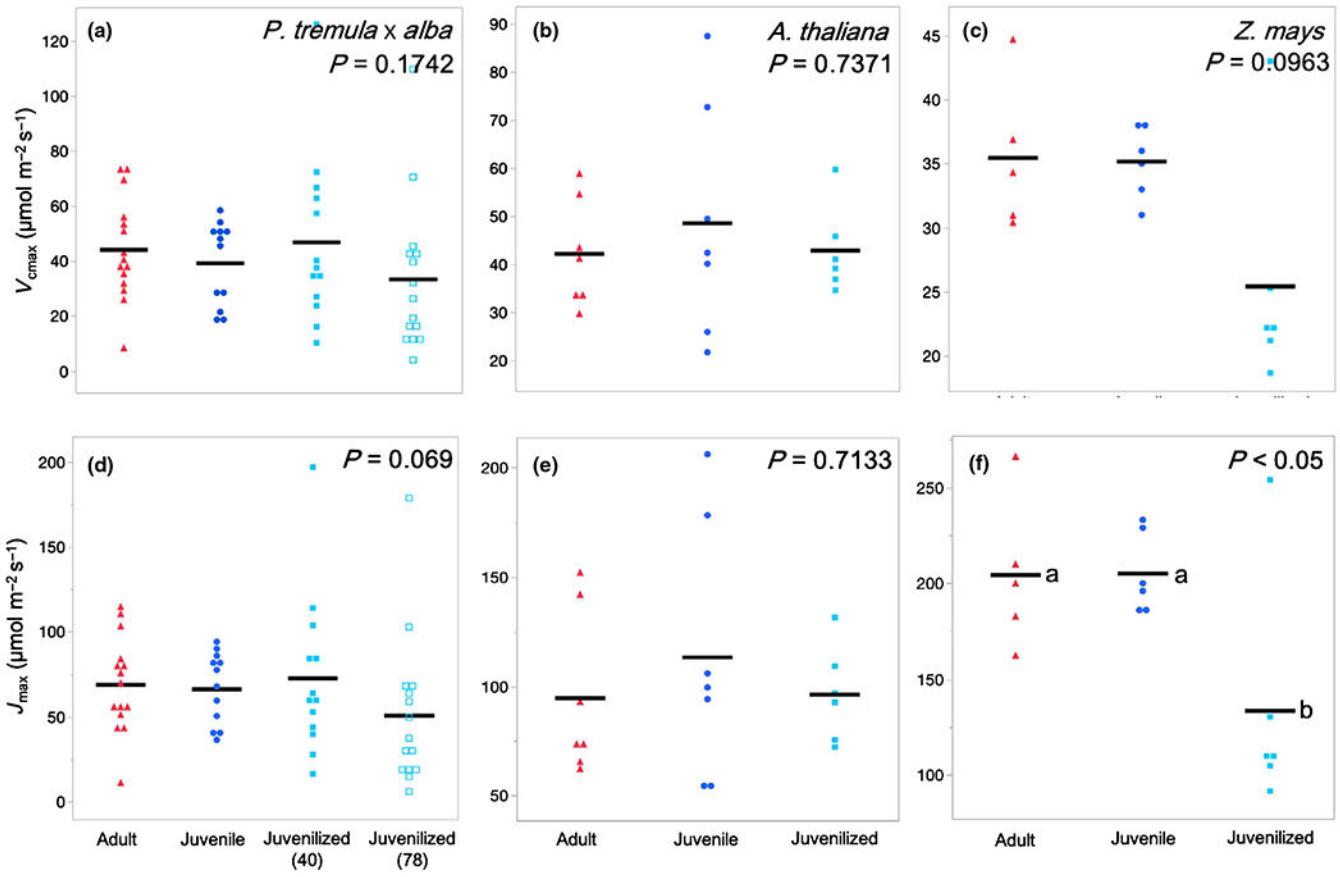

Fig. 6.

Maximum Rubisco carboxylation rate V_{cmax} and maximum electron transport rate for ribulose-1,5-bisphosphate regeneration J_{max} of adult (red triangles), juvenile (blue circles), and juvenilized (light blue closed or open squares) leaves of (a, d) *Populus tremula* × *alba*, (b, e) *Arabidopsis thaliana*, and (c, f) *Zea mays*. Means presented as black horizontal lines. *P*-values from one-way ANOVA with development as the main effect. For traits with significant ANOVA results ($P < 0.05$), different lower-case letters indicate means of developmental stage are significantly different according to Student's *t*-test ($P < 0.05$).

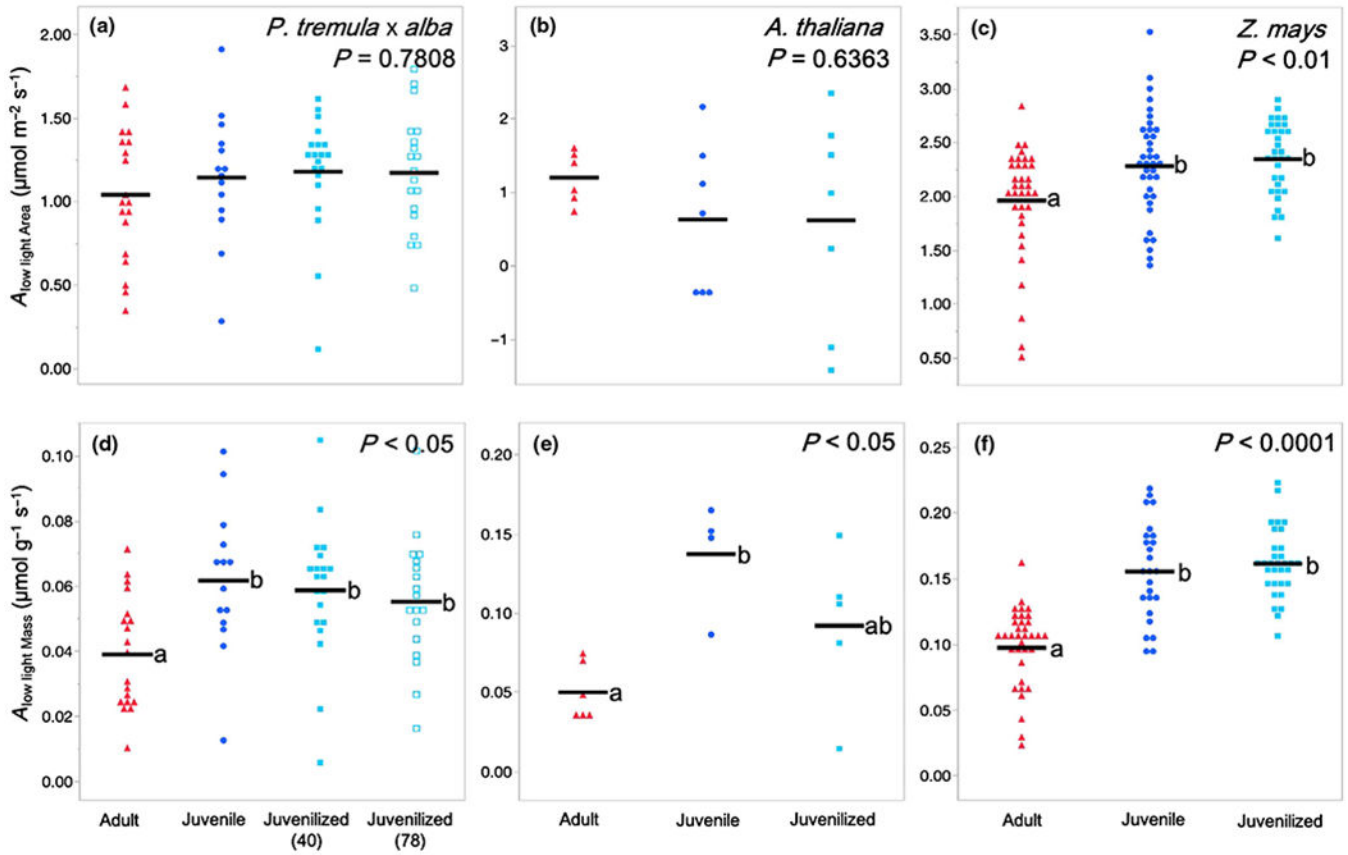

Fig. 7.

Low-light photosynthetic rates for (a, d) *Populus tremula* × *alba*, (b, e) *Arabidopsis thaliana*, and (c, f) *Zea mays*. Light levels were approximately two to three times the light compensation point at 25 μmol m^{-2} s^{-1} for *P. tremula* × *alba* and *A. thaliana* or 50 μmol m^{-2} s^{-1} for *Z. mays*. Traits depicted are (a–c) area-based net photosynthetic rate at low light $A_{\text{low light Area}}$ and (d–f) mass-based net photosynthetic rate at low light $A_{\text{low light Mass}}$. Leaf developmental phase represented as adult (red triangles), juvenile (blue circles), and juvenilized (light blue closed or open squares). Means presented as black horizontal lines. *P*-values from one-way ANOVA with development as the main effect. For traits with significant ANOVA results ($P < 0.05$), different lower-case letters indicate means of developmental stage are significantly different according to Student's *t*-test ($P < 0.05$).

Table 1

Photosynthetic nitrogen use efficiency represented by the slope of the linear relationship between mass-based light-saturated photosynthetic rate $A_{\text{sat Mass}}$ and mass-based leaf nitrogen N_{mass}.

Species	Effect	Slope	*y*-intercept	r^2	*P*-value
Populus tremula × alba	All stages	0.25	−0.30	0.55	< 0.0001
	N_{mass} × Developmental stage				0.8654
Arabidopsis thaliana	All stages	ns	ns	ns	ns
	N_{mass} × Developmental stage				ns
Zea mays	All stages	0.42	−0.11	0.50	< 0.0001
	N_{mass} × Developmental stage				0.1626

Variation in leaf nitrogen was too low to find any significant relationship in *Arabidopsis thaliana* (ns, not significant). *P*-values determined by least-squares linear regression analysis across all leaves and by ANCOVA with developmental stage as the covariate.

Table 2

Photosynthetic and leaf morphological traits for juvenile and adult leaves of *Populus tremula* × *alba* grown from seed.

Trait	Developmental stage	Mean ± SE	*n*	Effect	df	*P*-value
SLA ($cm^2\ mg^{-1}$)	Adult	0.20 ± 0.01	20	Developmental stage	1	< 0.001
	Juvenile	0.25 ± 0.01	34	Leaf position	1	< 0.05
$A_{sat\ Area}$ ($\mu mol\ m^{-2}\ s^{-1}$)	Adult	13.81 ± 0.69	20	Developmental stage	1	< 0.05
	Juvenile	10.32 ± 0.71	39	Leaf position	1	< 0.001
$A_{sat\ Mass}$ ($\mu mol\ m^{-2}\ s^{-1}$)	Adult	0.026 ± 0.002	20	Developmental stage	1	0.6039
	Juvenile	0.020 ± 0.001	33	Leaf position	1	< 0.1126
V_{cmax} ($\mu mol\ m^{-2}\ s^{-1}$)	Adult	52.48 ± 4.03	20	Developmental stage	1	0.3886
	Juvenile	35.71 ± 2.56	37	Leaf position	1	< 0.01
J_{max} ($\mu mol\ m^{-2}\ s^{-1}$)	Adult	84.34 ± 6.74	20	Developmental stage	1	0.3918
	Juvenile	56.91 ± 3.87	37	Leaf position	1	< 0.01
g_s high light ($mol\ m^{-2}\ s^{-1}$)	Adult	0.206 ± 0.017	20	Developmental stage	1	0.4312
	Juvenile	0.181 ± 0.011	39	Leaf position	1	0.8840
$A_{low\ light\ Area}$ ($\mu mol\ m^{-2}\ s^{-1}$)	Adult	0.79 ± 0.10	20	Developmental stage	1	0.5738
	Juvenile	1.04 ± 0.05	39	Leaf position	1	0.9723
$A_{low\ light\ Mass}$ ($\mu mol\ m^{-2}\ s^{-1}$)	Adult	0.002 ± 0.0003	20	Developmental stage	1	0.9623
	Juvenile	0.002 ± 0.0002	33	Leaf position	1	0.8233
g_s low light ($mol\ m^{-2}\ s^{-1}$)	Adult	0.102 ± 0.012	20	Developmental stage	1	0.6891
	Juvenile	0.139 ± 0.011	39	Leaf position	1	0.9723
Φ	Adult	0.057 ± 0.003	20	Developmental stage	1	0.4110
	Juvenile	0.053 ± 0.002	39	Leaf position	1	0.1068
LCP ($\mu mol\ m^{-2}\ s^{-1}$)	Adult	14.46 ± 1.40	20	Developmental stage	1	0.6686
	Juvenile	8.61 ± 0.63	39	Leaf position	1	0.1916
F_v/F_m	Adult	0.78 ± 0.008	20	Developmental stage	1	< 0.05
	Juvenile	0.77 ± 0.007	39	Leaf position	1	< 0.01
ΦPSII	Adult	0.120 ± 0.010	20	Developmental stage	1	0.1680
	Juvenile	0.092 ± 0.008	39	Leaf position	1	< 0.01
NPQ	Adult	4.90 ± 1.03	20	Developmental stage	1	0.6039

Trait	Developmental stage	Mean ± SE	*n*	Effect	df	*P*-value
	Juvenile	5.75 ± 0.64	39	Leaf position	1	0.8400
ETR (μmol m^{-2} s^{-1})	Adult	78.58 ± 6.63	20	Developmental stage	1	0.1680
	Juvenile	60.48 ± 5.42	39	Leaf position	1	< 0.01
R_{day} (μmol m^{-2} s^{-1})	Adult	−1.09 ± 0.16	20	Developmental stage	1	0.3886
	Juvenile	−0.78 ± 0.12	39	Leaf position	1	< 0.05

P-values from one-way ANOVA with developmental stage or leaf position as the effect variable. $A_{low\ light}$, low-light net photosynthesis; A_{sat}, light-saturated photosynthetic rate; ETR, electron transport rate; g_s, stomatal conductance; J_{max}, maximum electron transport rate for ribulose-1,5-bisphosphate regeneration; LCP, light compensation point; NPQ, non-photochemical quenching; PSII, photosystem II; R_{day}, day respiration; SLA, specific leaf area; V_{cmax}, maximum rate of Rubisco carboxylation.

Table 3

Linear fit between mass-based low-light photosynthetic rates ($A_{\text{low light Mass}}$) and specific leaf area (SLA).

Species	Traits	Slope	*y*-intercept	r^2	*P*-value
Populus tremula × alba	$A_{\text{low light Mass}}$ vs SLA	1.52×10^{-4}	−0.017	0.408	< 0.0001
Arabidopsis thaliana	$A_{\text{low light Mass}}$ vs SLA	9.851×10^{-5}	0.02	0.382	< 0.05
Zea mays	$A_{\text{low light Mass}}$ vs SLA	2.89×10^{-4}	−0.04	0.576	< 0.0001